Cancer Management and Research

Dovepress

open access to scientific and medical research

Open Access Full Text Article

ORIGINAL RESEARCH

Circ_0015756 Aggravates Hepatocellular Carcinoma Development by Regulating FGFR1 via Sponging miR-610

This article was published in the following Dove Press journal:
Cancer Management and Research

Weisheng Guo[1]
Lin Zhao[1]
Guangya Wei[1]
Peng Liu[1]
Yu Zhang[1]
Liran Fu[2]

[1]Department of Hepatobiliary Surgery, Henan Province Hospital of Traditional Chinese Medicine, The Second Affiliated Hospital of Henan University of Traditional Chinese Medicine, Zhengzhou, Henan 450002, People's Republic of China; [2]Department of Traditional Chinese Medicine, People's Hospital of Zhengzhou, Zhengzhou, Henan 450000, People's Republic of China

Background: Hepatocellular carcinoma (HCC) is the leading threat of cancer-related death in humans. Increasing studies show that circular RNAs (circRNAs) are important indicators in cancer diagnosis and prognosis. This study intended to explore the function and mechanism of circ_0015756 in HCC, providing the additional opinion for HCC treatment.

Materials and Methods: Quantitative real-time polymerase chain reaction (qRT-PCR) was utilized to detect the expression of circ_0015756 and miR-610. Cell viability was assessed by cell counting kit-8 (CCK-8) assay, and colony formation capacity was ascertained by colony formation assay. Cell migration and invasion were monitored by transwell assay. Cell cycle progression and apoptosis were analyzed by flow cytometry assay. Circ_0015756 oncogenicity was determined by Xenograft models. The targets of circ_0015756 and miR-610 were predicted by bioinformatics tools and validated using RNA pull-down, RNA immunoprecipitation (RIP) and dual-luciferase reporter assays. The expression level of fibroblast growth factor receptor 1 (FGFR1) was measured by Western blot.

Results: The expression of circ_0015756 was increased in HCC tissues, serums and cells. Circ_0015756 downregulation impaired HCC cell viability, colony formation capacity, invasion and migration, induced cell cycle arrest and apoptosis, and inhibited tumor growth in vivo. MiR-610 was ensured as a target of circ_0015756, and miR-610 absence reversed the effects of circ_0015756 downregulation. Further, FGFR1 was targeted by miR-610, and FGFR1 overexpression overturned the effects of miR-610 restoration in HCC cells. Circ_0015756 could regulate FGFR1 expression by targeting miR-610.

Conclusion: Circ_0015756 played its tumorigenic properties in HCC by activating FGFR1 via sponging miR-610, and circ_0015756 was expected to be a vital indicator in HCC diagnosis and treatment.

Keywords: circ_0015756, miR-610, FGFR1, HCC

Introduction

Hepatocellular carcinoma (HCC) constitutes most of the primary liver cancers and is the most common cause of cancer-related death.[1] Viral hepatitis and cirrhosis are the leading risk factors for HCC, but the exact mechanism of their occurrence is unknown.[2] In addition, fatty liver disease caused by diabetes and obesity has been recognized as an important risk factor for HCC, and multiple risk factors may work together to promote the occurrence of HCC.[3,4] Early treatment options for HCC with curative potential include surgical resection, ablation, and liver transplantation.[2,5] However, 40~70% of patients eventually relapse within 5 years.[6] HCC has a poor

Correspondence: Liran Fu
Department of Traditional Chinese Medicine, People's Hospital of Zhengzhou, Zhengzhou, Henan 450000, People's Republic of China
Tel +86- 15837117112
Email rbj9laz@163.com

submit your manuscript | www.dovepress.com
DovePress
http://doi.org/10.2147/CMAR.S262231

prognosis, and the prevention and treatment of HCC are still difficult tasks. Therefore, exploring the pathogenesis of HCC from multiple levels and perspectives is helpful in improving the treatment plan and the effect of HCC.

Circular RNAs (circRNAs), belonging to non-coding RNAs (ncRNAs), are a class of closed-loop RNA molecules that are arisen from precursor mRNA back-splicing or skipping events.[7] High-throughput sequencing and quantification methods are the main ways to detect circRNAs,[8] and the consequence suggests that the level of certain circRNAs is highly specific to cell or tissue type and developmental stage.[9] Accumulating evidence insists that circRNAs play a crucial function in human cancers.[7,10] Several circRNAs are expressed with an aberrant level in pathological conditions in a tissue or cell-specific manner, such as circ_0001955, circ_0000204 and circ_0091570 in HCC.[11–13] They functioned as important regulators in cancer cellular activities, including proliferation, metastasis and death. From a circRNA expression profiling, we obtained that circ_0015756, derived from complement factor H (CFH), was one of the highly expressed signatures in hepatoblastoma tissues compared to adjacent normal tissues,[14] and the investigations in its functions and associated action mechanism are deficient.

MicroRNAs (miRNAs), a cluster of ncRNAs with short nucleotides in length, have been researched hotspots for a long time. The association between miRNAs and cancer has been widely mentioned in different types of cancer, and miRNAs are served as treasures for cancer diagnosis, treatment and prognosis.[15–17] MiR-610 is a limitedly researched miRNA, and we acknowledge from a previous study that underexpression of miR-610 promoted tumorigenesis and development of HCC, indicating the essential role of miR-610 in HCC.[18] However, the relevant action mechanism of miR-610 in HCC is insufficient and needs further exploration.

MiRNAs are accustomed to inhibit mRNA expression and function by binding to specific sequences of 3′untranslated region (3′UTR) of downstream mRNAs, thus exerting their biological functions.[19] Fibroblast growth factor receptor 1 (FGFR1), a member of receptor tyrosine kinases, regulates various biological processes.[20] FGFR1 participated in the pathogenesis of diverse cancers by acting as a target of miRNAs, such as miR-133b in osteosarcoma[21] or miR-802 in non-small cell lung cancer.[22] Nevertheless, the similar regulatory mechanism of FGFR1 in HCC is limited.

In brief, the expression of circ_0015756 was ascertained in HCC tissues, serum and cells. Loss-function experiments were designed to determine the role of circ_0015756 in HCC in vitro and in vivo. Also, through the prediction and analysis of targets, the circ_0015756/miR-610/FGFR1 regulatory axis was constructed to partly explain the mechanisms of HCC development.

Materials and Methods

Clinical Sample Collection

HCC patients and healthy volunteers were recruited from Henan Province Hospital of Traditional Chinese Medicine. HCC tissues (n=32) and matched surrounding normal tissues (n=32) were obtained from HCC patients, and HCC serum specimens (n=32) and normal serum specimens (n=26) were obtained from HCC patients and healthy volunteers, respectively. These fresh tissues and serums were frozen and stored at −80°C conditions until further use. Prior patient's informed consent was signed, and this research acquired the approval from the Institute Research Ethics Committee of Henan Province Hospital of Traditional Chinese Medicine.

Cell Lines

Two HCC cell lines, including SNU-387 and Huh7, and immortalized human hepatocytes (THLE-2) were purchased from YaJi Biological (Shanghai, China). SNU-387 cells were cultured in Roswell Park Memorial Institute (RPMI-1640; Gibco, Carlsbad, CA, USA) containing 10% fetal bovine serum (FBS). Huh7 cells were kept in Dulbecco's Modified Eagle Medium (DMEM; Gibco) supplemented with 10% FBS.

THLE-2 cells were maintained in Bronchial Epithelial Cell Growth Medium (BEGM; Gibco) containing 10% FBS. All cells were maintained in a thermostatic incubator at a constant temperature of 37°C with moist air and 5% CO_2.

Circular Structure Analysis

The sequence of circ_0015756 was obtained from circbank (http://www.circbank.cn/), and then the sequence was further analyzed by the Genome Browser tool (https://genome.ucsc.edu/), including back-splicing site and exon regions.

Cell Transfection

We used small interference RNA (siRNA) to decrease circ_0015756 expression. SiRNA targeting circ_0015756

(si-circ_0015756-1 and si-circ_0015756-2) plus its negative control (si-NC), miR-610 mimic plus its negative control (miRNA NC) and miR-610 inhibitor plus its negative control (inhibitor NC) were all synthesized by Ribobio Co. Ltd (Guangzhou, China). For FGFR1 overexpression, FGFR1 sequence was cloned into pcDNA overexpression vector, generating FGFR1 overexpression vector (pc-FGFR1), and empty pcDNA was served as a negative control (pc-NC). Construction of expression vector was accomplished by Sangon Biotech (Shanghai, China). These transfection contents were introduced into SNU-387 and Huh7 cells using Lipofectamine 3000 (Invitrogen, Carlsbad, CA, USA).

Quantitative Real-Time Polymerase Chain Reaction (qRT-PCR)

Total RNA was isolated using TRIzol reagent (Qiagen, Duesseldorf, Germany). For circRNA and mRNA analysis, PrimeScript RT Master Mix (Takara, Tokyo, Japan) and TB Green Premix Ex Taq (Takara) were used for reverse transcription and qRT-PCR, with glyceraldehyde-3-phosphate dehydrogenase (GAPDH) as the housekeeping gene. For miRNA analysis, miScript reverse transcription kit (Qiagen), and miScript SYBR Green PCR kit (Qiagen) were utilized, with U6 as the housekeeping gene. The relative expression was calculated using the $2^{-\Delta\Delta Ct}$ method, and all used primers were listed as below: circ_0015756, F: 5′-AATGGATGGAGCCAGTAA-3′ and R: 5′-AAACCACCCTCACAAGTA-3′; CFH, F: 5′-CAGCAGTACCATGCCTCAGA-3′ and R: 5′-GGATGCATCTGGGAGTAGGA-3′; miR-610, F: 5′-AGAAGGCTGGGGCTCATTTG-3′ and R: 5′-AGGGGCCATCCACAGTCTTC-3′; FGFR1, F: 5′-CCTGGTGACAGAGGACAATG-3′ and R: 5′-AGATCCGGTCAAATAATGCC-3′; GAPDH, F: 5′-GACTCAT GACCACAGTCCATGC-3′ and R: 5′-AGAGGCAGGGATGATGTTCTG-3′; U6, F: 5′-CTCGCTTCGGCAGCACA-3′ and R: 5′-AACGCTTCACGA ATTTGCGT-3′.

Cell Counting Kit-8 (CCK-8) Assay

CCK-8 assay kit (Beyotime, Shanghai, China) was used to examine cell viability. Briefly, transfected cells were seeded into 96-well plates (2×10^3 cells/well). After 24 h post-transfection, 10 μL CCK-8 reagent was pipetted into every well, reacting for another 2 h. The absorbance at 450 nm was measured by the microplate reader (BioTek, Winooski, VT, USA).

Colony Formation Assay

Cells with transfection were incubated for 24 h, and then cells (200 cells/well) were digested with trypsin and replanted into 10 cm^2 plate. After culturing for 2 weeks, cells were subjected to methanol and 0.1% crystal violet. Colonies larger than 100 μm in diameter were counted under a microscope (Olympus, Tokyo, Japan).

Transwell Assay

SNU-387 and Huh7 cells (3×10^4) with transfection in serum-free culture medium were transferred into the upper chambers (BD Biosciences, San Jose, CA, USA) for migration analysis or chambers pre-treated with Matrigel (BD Biosciences) for invasion analysis. Meanwhile, the bottom of chambers was padded with corresponding fresh culture medium (containing 10% FBS). Over the next 24 h, cells in 37°C conditions were allowed to migrate and invade. The migrated or invaded cells in the lower surface were fixed with methanol and dyed with 0.1% crystal violet, followed by observation under a microscope (100 × magnification; Olympus).

Cell Cycle Distribution and Cell Apoptosis Analyses

SNU-387 and Huh7 cells with transfection were seeded into 6-well plates (2×10^5 cells/well). After culturing for 24 h, cell cycle was detected using cell cycle analysis kit (Vybrant DyeCycle; Invitrogen) in line with the manufacturer's guideline and analyzed by flow cytometry using Attune™ NxT Acoustic Focusing Cytometer (Invitrogen).

SNU-387 and Huh7 cells with transfection for 48 h were collected and washed with phosphatic buffer saline (PBS). Then, cells (6×10^4) were used to conduced apoptosis analysis using the Annexin V-FITC and PI Apoptosis Detection Kit (FITC: fluorescein isothiocyanate; PI: propidium iodide) (Beyotime) following the protocol. The apoptotic cells were analyzed by flow cytometry using Attune™ NxT Acoustic Focusing Cytometer (Invitrogen).

In vivo Experiments

For circ_0015756 stable downregulation, short hairpin RNA lentiviral vector containing circ_0015756 (sh-circ_0015756) and its negative control (sh-NC) were assembled by Sangon Biotech. In Xenograft models, Huh7 cells infected with lentivirus vector-packaged sh-circ_0015756 or sh-NC were implanted into the right side of the nude mice (4~6 weeks-old, BALB/c, n=10)

purchased from Charles River (Beijing, China). All the nude mice were housed in the specific pathogen-free animal room. After housing for 1 week, tumor volume was recorded once a week, and tumor weight was measured after 28 d when mice were killed. All animal experiments were carried out with the approval of the Animal Care and Use Committee of Henan Province Hospital of Traditional Chinese Medicine and followed the guidelines of the Guide for the Care and Use of Laboratory Animals (GB/T 35892-2018; Standardization Administration of the People Republic of China).

Target Gene Prediction

The online bioinformatics tool circRNA interactome (https://circinteractome.nia.nih.gov/) was used to predict the targets of circ_0015756, and another bioinformatics tool Targetscan (http://www.targetscan.org/vert_72/) was used to predict the targets of miR-610.

RNA Pull-Down Assay

The sequence of mutations in miR-610 at the binding site with circ_0015756 was designed, named as MUT-miR-610. Then, miR-610, miRNA NC and MUT-miR-610 were subjected to biotinylation in Ribobio Co. Ltd., terming as biotin-miR-610 mimic, biotin-miRNA NC and biotin-miR-610 mimic MUT. Then, all of them were individually transfected into SNU-387 and Huh7 cells. After 48 h, transfected cells were lysed, and cell lysates were incubated with Dynabeads MyOne Streptavidin beads (Invitrogen). Subsequently, RNA was extracted using TRIzol Reagent (Qiagen) from the beads and detected by qRT-PCR.

RNA Immunoprecipitation (RIP) Assay

SNU-387 and Huh7 cells were transfected with miR-610 mimic, miR-610 mimic MUT or miRNA NC. Transfected cells were then lysed, and cell lysates were subjected to RIP buffer mixed with magnetic beads coated with Argonaute 2 antibody (anti-Ago2) or Immunoglobulin G antibody (anti-IgG; control). After sufficient mixing and washing, the complexes on beads were analyzed using qRT-PCR.

Dual-Luciferase Reporter Assay

The sequence fragment of circ_0015756 containing miR-610 binding site and the corresponding mutant sequence fragment were synthesized and inserted into the pmirGLO expression vector (Promega, Madison, WI, USA), namely WT-circ_0015756 and MUT-circ_0015756. Similarly, WT-FGFR1 3′UTR and MUT-FGFR1 3′UTR were also generated following the same manner. Subsequently, SNU-387 and Huh7 cells were cotransfected with miR-610 mimic and WT-circ_0015756, MUT-circ_0015756, WT-FGFR1 3′UTR or MUT-FGFR1 3′UTR, and miRNA NC and these fusion plasmids were also cotransfected into SNU-387 and Huh7 cells as the control. After 48 h-transfection, the luciferase activity of cells was measured using the Dual-Luciferase Assay System (Promega).

Western Blot

Protein samples were prepared and detected using the BCA protein assay kit (Beyotime). Then, an equal amount (20 μg) of protein was used in the Western blot analysis. The primary antibodies used were anti-FGFR1 (ab76464; Abcam, Cambridge, MA. USA) and GAPDH (ab9485; Abcam). The secondary antibody used was anti-Goat anti-Rabbit (ab205718; Abcam). The protein blots were emerged using an enhanced chemiluminescence (ECL) kit (Beyotime).

Statistical Analysis

All data were collected from three groups of independent experiments and showed as mean ± standard deviation. Statistical analyses were performed using GraphPad Prism 5 software (San Diego, CA, USA). Comparisons between two groups were executed using Student's *t* tests, and comparisons among three or more groups were conducted using analysis of variance with Tukey post-hoc test. Statistical differences were defined as $P < 0.05$.

Result

Circ_0015756 Was Significantly Up-Regulated in HCC Tissues, Serum and Cells

To ensure the expression pattern of circ_0015756 in HCC, we detected the expression of circ_0015756 in tissues, serum and cells. The result showed that the expression of circ_0015756 was significantly increased in tumor tissues compared to adjacent normal tissues from HCC patients (Figure 1A). Besides, circ_0015756 expression was also notably elevated in serum from HCC patients compared with that from normal subjects (Figure 1B). In addition, circ_0015756 expression was enhanced in SNU-387 and Huh7 compared to THLE-2 cells (Figure 1C). Through bioinformatics analysis, we predicted the formation mode

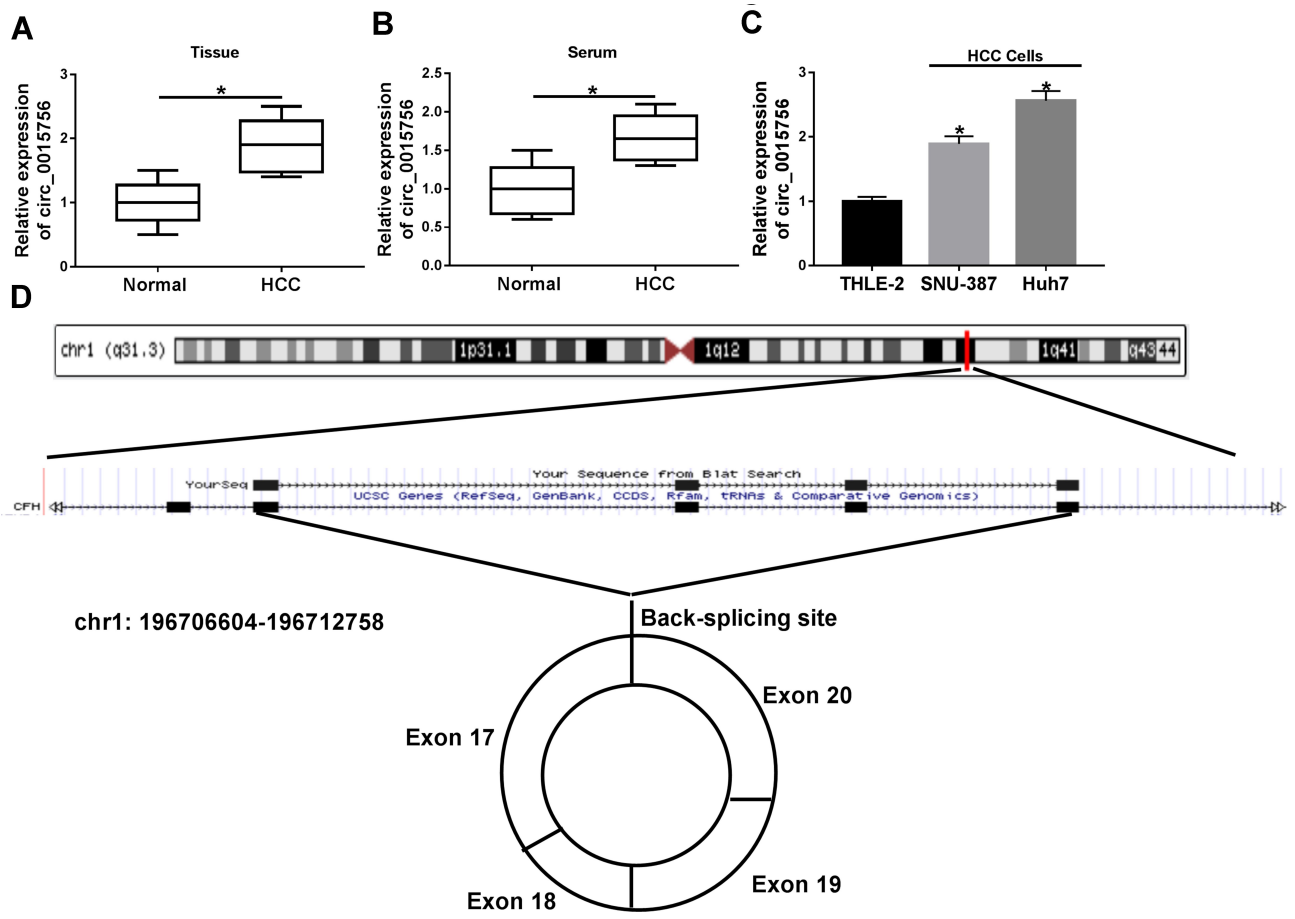

Figure 1 The expression of circ_0015756 was increased in HCC tissues, serum and cells. The expression of circ_0015756 in (**A**) tissues, (**B**) serum, and (**C**) cell lines was detected by qRT-PCR. (**D**) The generation form of circ_0015756 was speculated through bioinformatics analysis. *$P < 0.05$.
Abbreviations: HCC, hepatocellular carcinoma; qRT-PCR, quantitative real-time polymerase chain reaction.

of circ_0015756 circular structure (Figure 1D). In total, circ_0015756 was aberrantly overexpressed in HCC, hinting that circ_0015756 affected HCC development.

Circ_0015756 Downregulation Blocked HCC Tumorigenesis and Development in vitro and in vivo

We used siRNA to knock down the expression of circ_0015756 in HCC cells. SNU-387 and Huh7 cells were transfected with si-circ_0015756 or si-NC, and qRT-PCR data showed that the expression of circ_0015756 was significantly decreased in transfected cells, while the expression of CFH mRNA was unaffected (Figure 2A). In function, circ_0015756 downregulation prominently diminished viability and colony formation ability of SNU-387 and Huh7 cells (Figure 2B and C), suggesting that cell proliferation was suppressed. The capacities of migration and invasion were also detected, and we found that circ_0015756 downregulation effectively reduced the number of migrated and invaded SNU-387 and Huh7 cells (Figure 2D and E). Moreover, cell cycle distribution suggested that the number of SNU-387 and Huh7 cells after circ_0015756 downregulation was suppressed from G0/G1 to S transition (Figure 2F), hinting that cell cycle was arrested. Furthermore, circ_0015756 downregulation significantly promoted apoptosis rate of SNU-387 and Huh7 cells (Figure 2G). Not surprisingly, in vivo mice experiment presented that the volume and weight of tumor tissues from the sh-circ_0015756 group were far less than that from the sh-NC group (Figure 2H and I), and the expression of circ_0015756 in tumors from the sh-circ_0015756 group was lower than that from the sh-NC group (Figure 2J), suggesting that circ_0015756 downregulation suppressed tumor growth in vivo. These functional analyses concluded that circ_0015756 downregulation impaired HCC tumorigenesis and development in vitro and in vivo.

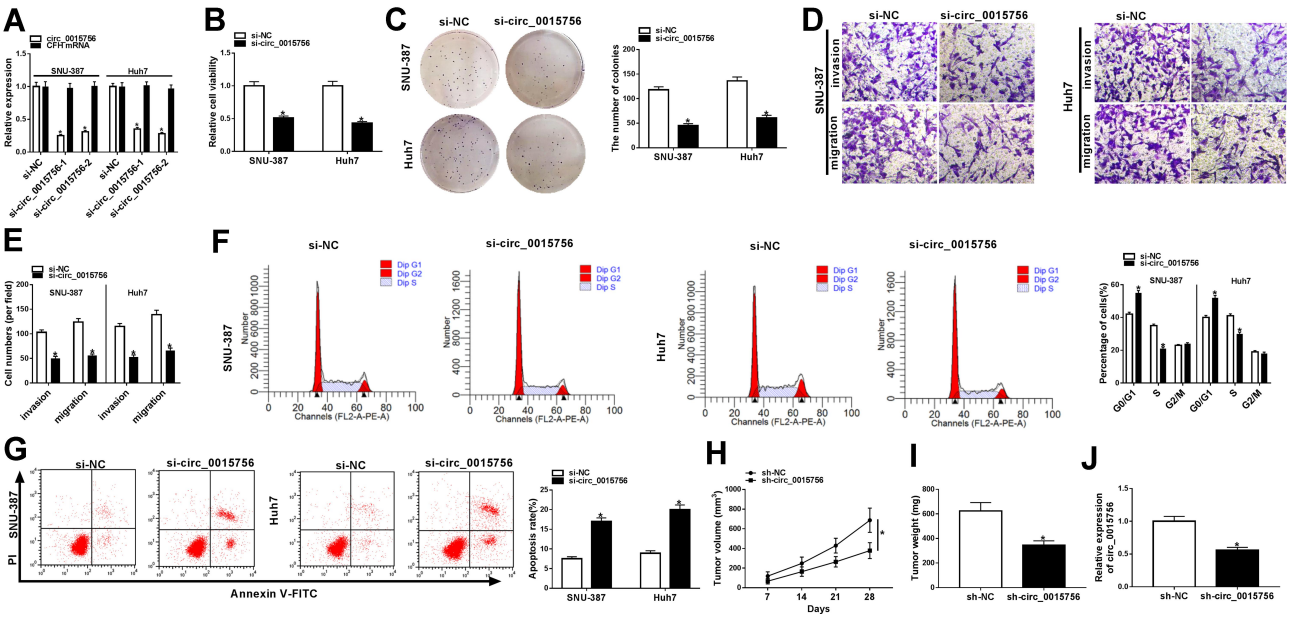

Figure 2 Circ_0015756 downregulation inhibited HCC cell viability, colony formation ability, migration and invasion, and induced cell cycle arrest and apoptosis. In SNU-387 and Huh7 cells transfected with si-circ_0015756 or si-NC, (**A**) the expression of circ_0015756 and its linear mRNA CFH was detected by qRT-PCR. (**B**) Cell viability was detected by CCK-8 assay. (**C**) Colony formation ability was assessed by colony formation assay. (**D** and **E**) Cell migration and invasion were monitored by transwell assay. (**F** and **G**) Cell cycle and apoptosis were examined by flow cytometry assay. (**H** and **I**) Tumor volume and weight were measured in Xenograft models. (**J**) The expression of circ_0015756 in Xenograft models was detected by qRT-PCR. *$P < 0.05$.

Abbreviations: NC, negative control; CFH, complement factor H; qRT-PCR, quantitative real-time polymerase chain reaction; FITC, fluorescein isothiocyanate; PI, propidium iodide.

Circ_0015756 Directly Bound to miR-610

Through the analysis of bioinformatics tool circRNA interactome, we found there was a targeting site between circ_0015756 and miR-610 sequence fragment, hinting that miR-610 might be a target of circ_0015756. To verify this prediction, the sequence at the binding site of circ_0015756 was mutated to generate a novel mutant sequence fragment (Figure 3A). Also, miR-610 sequence was randomly mutated at the binding site of circ_0015756 (Figure 3B). The result from biotin-labeled RNA pull-down assay indicated that circ_0015756 could be pulled down by biotin-miR-610 mimic rather than biotin-miRNA NC, and biotin-miR-610 mimic MUT could not pull down circ_0015756 in SNU-387 and Huh7 cells (Figure 3C and D). Additionally, the data from RIP assay presented that miR-610 mimic could enrich the abundance of circ_0015756 in the Ago2 RIP relative to that in the IgG RIP, while miR-610 mimic MUT could not lead to the same effects (Figure 3C and D). Moreover, dual-luciferase reporter assay showed that miR-610 mimic reintroduction significantly reduced the luciferase activity in SNU-387 and Huh7 cells pre-transfected with WT-circ_0015756 but not MUT-circ_0015756 compared to miRNA NC reintroduction (Figure 3E and F). The expression of miR-610 was impaired by the transfection of miR-610 inhibitor in SNU-387 and Huh7 cells (Figure 3G), and its expression was elevated in cells transfected with si-circ_0015756 but weakened in cells transfected with si-circ_0015756 +miR-610 inhibitor (Figure 3H). Overall, miR-610 was a target of circ_0015756.

MiR-640 Inhibition Reversed the Effects of Circ_0015756 Downregulation

Rescue experiments were performed in SNU-387 and Huh7 cells by transfecting with si-circ_0015756 or si-circ_0015756+miR-610 inhibitor, si-NC or si-circ_0015756 +inhibitor NC serving as a respective control. Cell viability was declined in cells transfected with si-circ_0015756 relative to si-NC while recovered in cells transfected with si-circ_0015756+miR-610 inhibitor relative to si-circ_0015756 +inhibitor NC (Figure 4A). The ability of colony formation was frustrated in cells with si-circ_0015756 transfection compared to si-NC transfection but restored in cells with si-circ_0015756+miR-610 inhibitor transfection compared to si-circ_0015756+inhibitor NC transfection (Figure 4B). The capacities of migration and invasion were depleted in SNU-387 and Huh7 cells after circ_0015756 knockdown, while

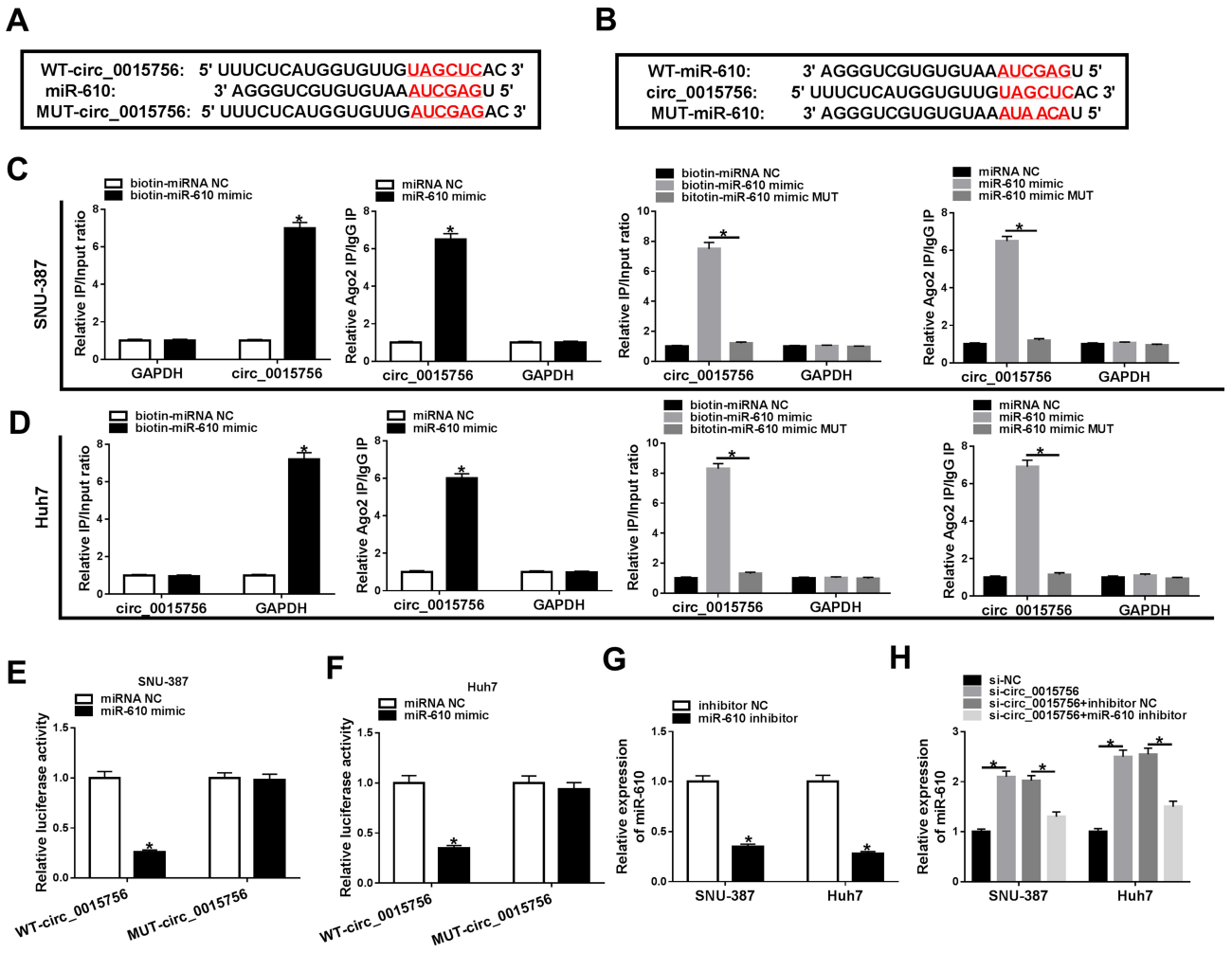

Figure 3 MiR-610 was a target of circ_0015756. (**A**) The binding site between circ_0015756 and miR-610 was analyzed by the bioinformatics tool circRNA interactome. (**B**) MiR-610 sequence was mutated at the binding site of circ_0015756. The interplay between circ_0015756 and miR-610 was verified by (**C** and **D**) RNA pull-down assay, (**C** and **D**) RIP assay and (**E** and **F**) dual-luciferase reporter assay. (**G**) The inhibitory efficiency of miR-610 was measured by qRT-PCR. (**H**) The expression of miR-610 in SNU-387 and Huh7 cells transfected with si-circ_0015756, si-NC, si-circ_0015756+miR-610 inhibitor or si-circ_0015756+inhibitor NC was checked by qRT-PCR. *$P < 0.05$.
Abbreviations: WT, wild-type; MUT, mutant-type; NC, negative control; GAPDH, glyceraldehyde-3-phosphate dehydrogenase; Ago2, argonaute 2; IgG, immunoglobulin G.

miR-610 absence recovered these capacities (Figure 4C and D). Cell cycle arrest caused by circ_0015756 downregulation was partly relieved by miR-610 absence in SNU-387 and Huh7 cells (Figure 4E and F). The apoptosis rate promoted in cells transfected with si-circ_0015756 was weakened in cells transfected with si-circ_0015756+miR-610 inhibitor (Figure 4G). In conclusion, circ_0015756 downregulation blocked HCC cell malignant development by enriching miR-610.

MiR-610 Suppressed HCC Cell Malignant Development by Binding to FGFR1

FGFR1 was one of the putative target mRNAs of miR-610 with a special binding site between its 3′UTR and miR-610, which was predicted by the bioinformatics tool Targetscan (Figure 5A). Dual-luciferase reporter assay showed that the luciferase activity in SNU-384 and Huh7 cells transfected with miR-610 mimic and WT-FGFR1 3′UTR was significantly decreased relative to miRNA NC but unaffected in cells transfected with MUT-FGFR1 3′UTR and miR-610 mimic or miRNA NC (Figure 5B). We also detected that the abundance of FGFR1 was increased in HCC tissues and cells compared with that in normal tissues and cells, respectively (Figure 5C and D). Subsequently, the efficiency of FGFR1 overexpression was checked, and the data showed that FGFR1 expression was highly enhanced in SNU-387 and Huh7 cells transfected with pc-FGFR1 compared to pc-NC (Figure 5E). Besides, the expression of FGFR1 was significantly impaired in SNU-387 and Huh7 cells transfected with

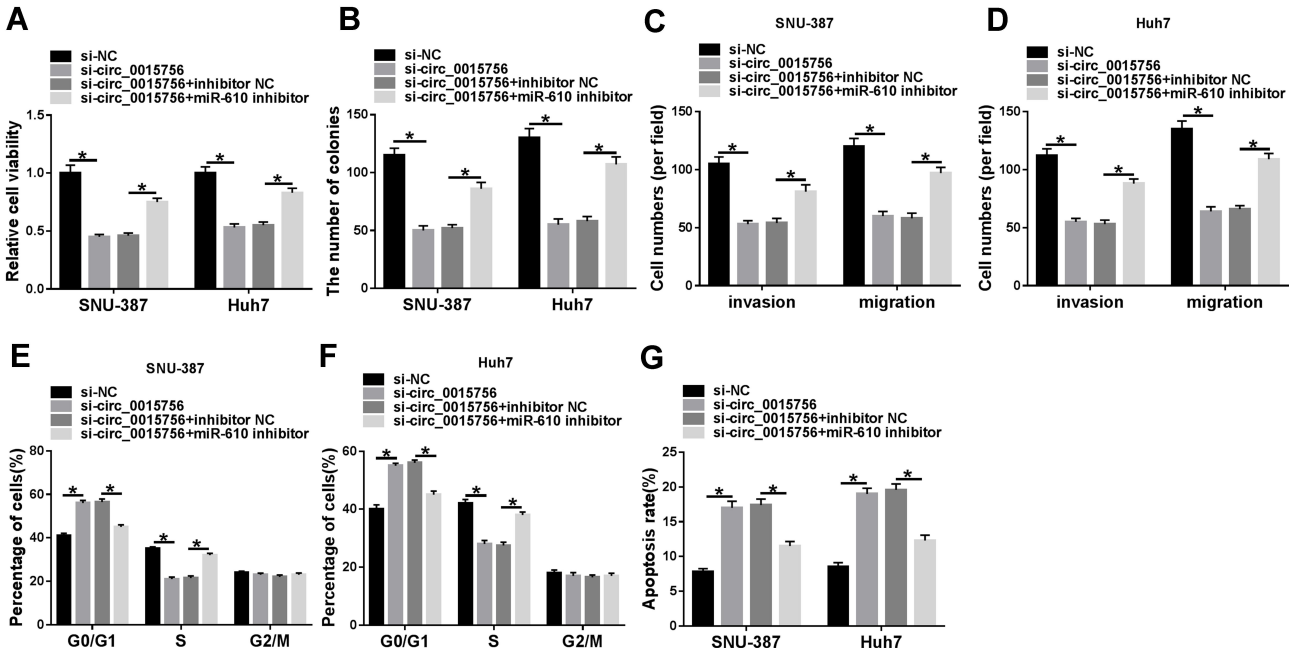

Figure 4 MiR-610 inhibition reversed the effects of circ_0015756 downregulation. In SNU-387 and Huh7 cells transfected with si-circ_0015756, si-NC, si-circ_0015756 +miR-610 inhibitor or si-circ_0015756+inhibitor NC, (**A**) cell viability was examined using CCK-8 assay. (**B**) The potency of colony formation was observed through colony formation assay. (**C** and **D**) The capacities of migration and invasion were investigated by transwell assay. (**E** and **F**) Cell cycle distribution was distinguished by flow cytometry assay. (**G**) Cell apoptosis was also monitored by flow cytometry assay. *$P < 0.05$.
Abbreviation: NC, negative control.

miR-610 mimic but recovered in cells transfected with miR-610 mimic+pc-FGFR1 (Figure 5F), suggesting that miR-610 bound to FGFR1 to suppress FGFR1 expression. The raw data of Western blot were exhibited in Supplemental Material. Functionally, cell viability and colony formation ability were substantially weakened in SNU-387 and Huh7 cells transfected with miR-610 mimic compared to miRNA NC but partly enhanced in cells transfected with miR-610 mimic+pc-FGFR1 compared to miR-610 mimic+pc-NC (Figure 5G and H). The transfection of miR-610 mimic in SNU-387 and Huh7 cells suppressed cell migration and invasion, while miR-610 mimic +pc-FGFR1 transfection induced cell migration and invasion (Figure 5I and J). Moreover, alone miR-610 overexpression in SNU-387 and Huh7 cells induced cell cycle arrest and cell apoptosis, while conjunct miR-640 and FGFR1 overexpression in SNU-387 and Huh7 cells blocked cell cycle arrest and cell apoptosis (Figure 5K–M). These findings maintained that miR-610 impaired FGFR1 expression to block HCC development in vitro.

Circ_0015756 Sponged miR-610 to Regulate FGFR1 Expression

Expression analysis was performed in specially transfected SNU-387 and Huh7 cells. As shown in Figure 6A, the expression of FGFR1 was significantly declined in cells transfected with si-circ_0015756, while FGFR1 expression was substantially recovered in cells transfected with si-circ _0015756+pc-FGFR1. As shown in Figure 6B, the expression of FGFR1 impaired by the transfection of si-circ _0015756 was partially strengthened by the transfection of si-circ_0015756+miR-610 inhibitor, indicating that circ_0015756 downregulation could weaken the level of FGFR1 by enhancing the level of miR-610.

Discussion

HCC is regarded as one of the most aggressive malignant tumors because of its outstanding metastasis potency.[23] The identification of target molecules associated with HCC pathogenesis has been regarded as a meritorious strategy,[24] and circRNAs are a class of potential targets with multiple available functions.[25]

In our study, we discovered that the expression of circ_0015756 was aberrantly strengthened in HCC tissues, serums and cells. We speculated that circ_0015756 might play an indispensable role in HCC development. The following functional experiments presented that circ_0015756 downregulation depleted HCC cell viability, colony formation capacity, migration and invasion, induced cell cycle arrest and apoptosis, and inhibited tumorigenesis and

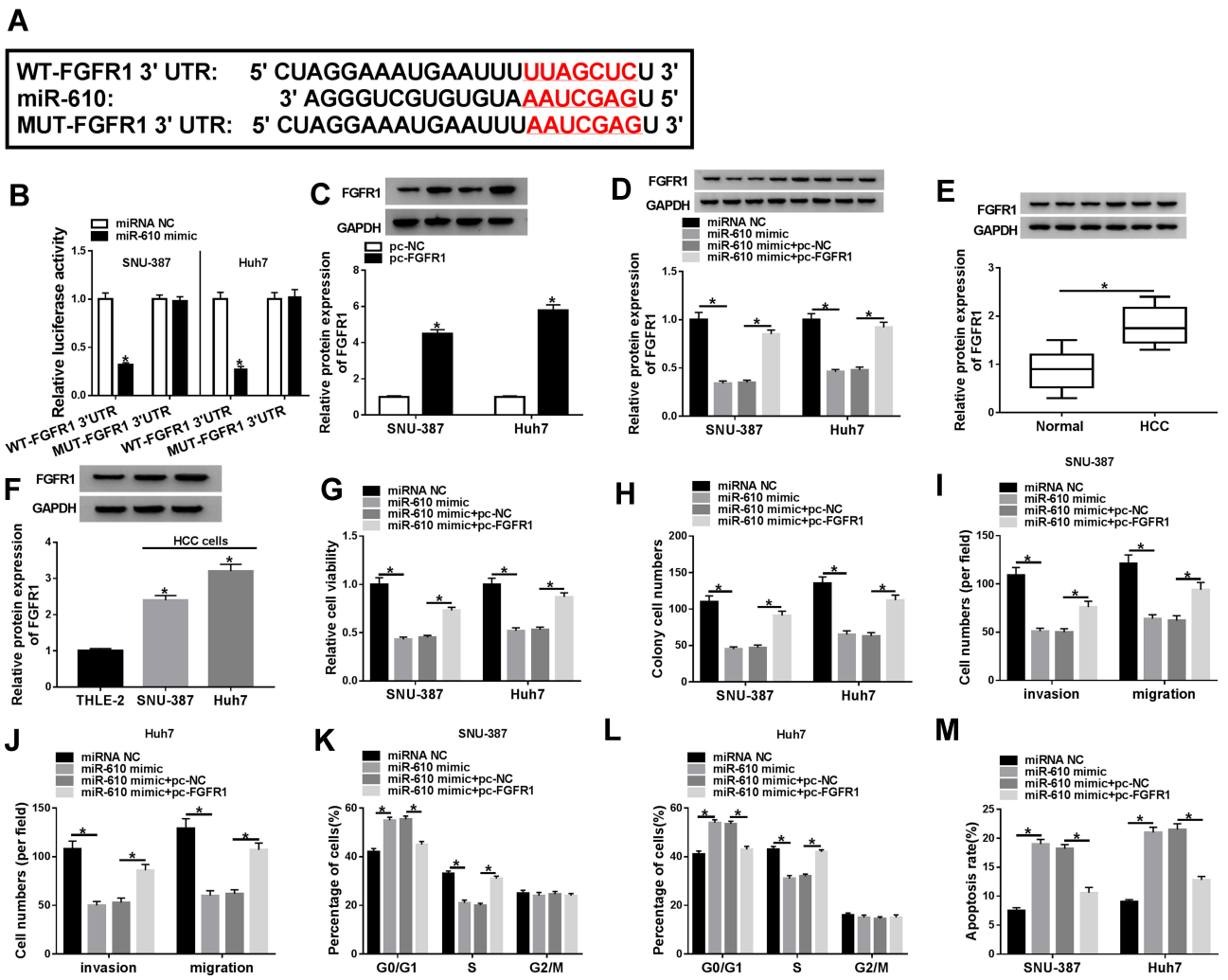

Figure 5 MiR-610 inhibited FGFR1 expression to block HCC malignant development in vitro. (**A**) The relationship and the binding site between miR-610 and FGFR1 were predicted by the bioinformatics tool Targetscan. (**B**) The interaction between miR-610 and FGFR1 was confirmed by dual-luciferase reporter assay. (**C**) The expression of FGFR1 in HCC tissues and normal tissues was detected by Western blot. (**D**) The expression of FGFR1 in HCC cells and normal cells was also measured by Western blot. (**E**) SNU-387 and Huh7 cells were transfected with pc-FGFR1 or pc-NC, and the transfection efficiency was detected according to FGFR1 expression using Western blot. In SNU-387 and Huh7 cells transfected with miR-610 mimic, miRNA NC, miR-610 mimic+pc-FGFR1 or miR-610 mimic+pc-NC, (**F**) the expression of FGFR1, (**G**) cell viability, (**H**) colony formation ability, (**I** and **J**) migration and invasion, (**K** and **L**) cell cycle distribution, and (**M**) cell apoptosis were examined by Western blot, CCK-8 assay, colony formation assay, transwell assay and flow cytometry assay, respectively. *$P < 0.05$.

Abbreviations: WT, wild-type; MUT, mutant-type; NC, negative control; pc, pcDNA; FGFR1, fibroblast growth factor receptor 1.

growth in vivo. These consequences implied that circ_0015756 possessed carcinogenic effects in HCC. Circ_0015756 was obtained from a circRNA expression profiling that distinguished differently expressed circRNAs between hepatoblastoma tissues and normal liver tissues.[14] Circ_0015756 was one of the significantly upregulated circRNAs in hepatoblastoma tissues, and circ_0015756 knockdown diminished viability, proliferation and invasion of hepatoblastoma cells.[14] Besides, a recent study proposed that circ_0015756 expression was elevated in cancerous liver tissues compared to noncancerous liver tissues, and cell migration was suppressed but cell apoptosis was promoted in HCC cells after circ_0015756 underexpression.[26] All these findings indicated that circ_0015756 played a carcinogenic role in HCC, and circ_0015756 knockdown could repress HCC development.

Previous studies documented that circ_0015756 functioned in HCC by adsorbing miR-1250-3p or miR-7,[14,26] suggesting that circ_0015756 was involved in cancer progression by acting as a miRNA sponge. Following this manner, we discovered that miR-610 was a target of circ_0015756, and circ_0015756 downregulation could strengthen the abundance of miR-610 in HCC cells. MiR-610 was found to be downregulated in HCC, and miR-610 deficiency accelerated cell proliferation and cell cycle progression, while miR-610 overexpression presented the

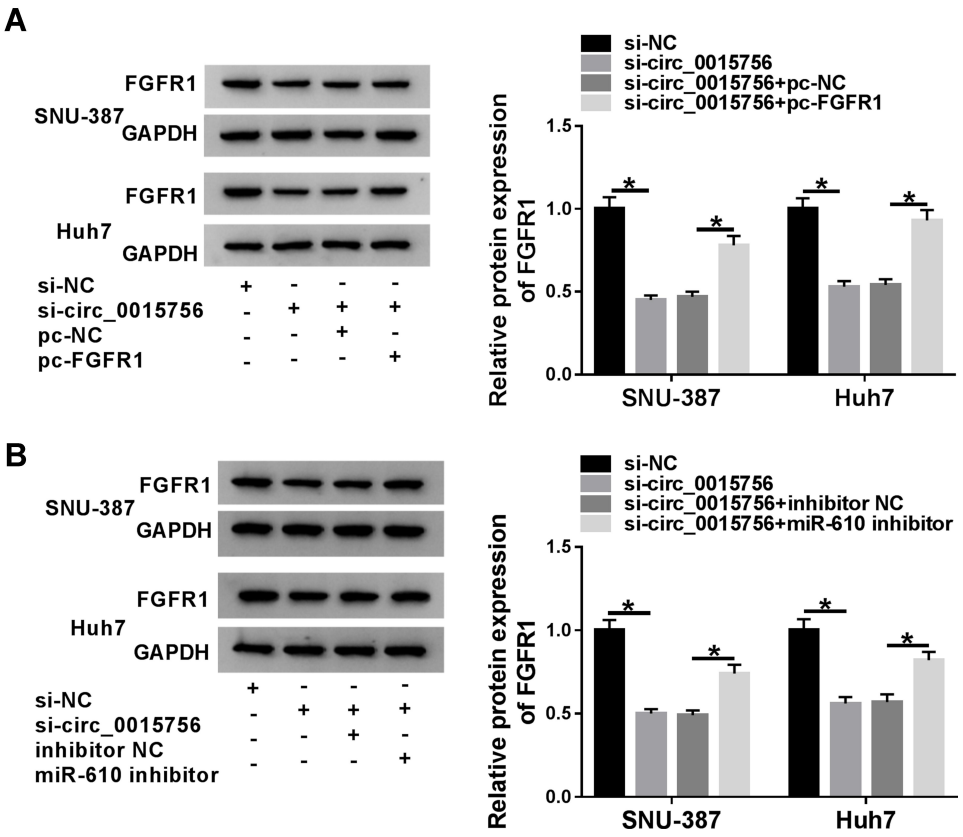

Figure 6 Circ_0015756 modulated FGFR1 expression by targeting miR-610. (**A**) SNU-387 and Huh7 cells were introduced with si-circ_0015756, si-NC, si-circ_0015756 +pc-FGFR1 or si-circ_0015756+pc-NC, and the expression of FGFR1 in these transfected cells was measured by Western blot. (**B**) SNU-387 and Huh7 cells were introduced with si-circ_0015756, si-NC, si-circ_0015756+miR-610 inhibitor or si-circ_0015756+inhibitor NC, and the expression of FGFR1 in these transfected cells was detected by Western blot. *$P < 0.05$.

Abbreviations: NC, negative control; pc, pcDNA; GAPDH, glyceraldehyde-3-phosphate dehydrogenase; FGFR1, fibroblast growth factor receptor 1.

opposite effects.[18] Interestingly, the expression of miR-610 was also mentioned to be depleted in colorectal cancer, gastric cancer and glioma,[27–29] and miR-610 played an anti-tumor role in these cancers. In our study, we demonstrated that miR-610 deficiency could reverse the effects of circ_0015756 downregulation, thus aggravating HCC deterioration, while miR-610 enrichment could block HCC progression.

Further analysis suggested that miR-610 combined with FGFR1 3′UTR through a special binding site, thus repressing FGFR1 expression. The function of FGFR1 in HCC has been largely uncovered in previous studies. For example, FGFR1 restoration promoted HCC cell proliferation and cell cycle progression but inhibited apoptosis.[30] Silencing Keratin 19 could weaken the expression of FGFR1, leading to the inhibition of HCC cell growth and the promotion of cell apoptosis.[31] Lenvatinib inhibited angiogenesis and induced cell death in HCC by suppressing FGFR signaling pathways or FGFR-MAPK cascades.[32,33] Consistent with these findings, we discovered that FGFR1 was highly expressed in HCC tissues and cells. Besides, FGFR1 overexpression abolished the effects of miR-610 enrichment, leading to HCC malignant development. Additionally, the expression of FGFR1 was decreased in HCC cells after circ_0015756 knockdown but enhanced in cells after circ_0015756 knockdown together with FGFR1 overexpression or miR-610 inhibition, suggesting that circ_0015756 regulated FGFR1 expression by targeting miR-610.

Conclusion

Our study concluded that circ_0015756 dysregulation was associated with HCC development, and circ_0015756 participated in HCC pathogenesis by regulating FGFR1 via sponging miR-610. Importantly, this study broadens the function of circ_0015756 in HCC and deepens understanding into HCC development, and circ_0015756 may be a promising biomarker or indicator in HCC treatment.

Funding

There is no funding to report.

Disclosure

The authors declare that they have no financial conflicts of interest.

References

1. Kulik L, EL-Serag HB. Epidemiology and management of hepatocellular carcinoma. *Gastroenterology*. 2019;156(2):477–491. doi:10.1053/j.gastro.2018.08.065
2. Yeh MM, Yeung RS, Apisarnthanarax S, et al. Multidisciplinary perspective of hepatocellular carcinoma: a Pacific Northwest experience. *World J Hepatol*. 2015;7(11):1460–1483. doi:10.4254/wjh.v7.i11.1460
3. Zoller H, Tilg H. Nonalcoholic fatty liver disease and hepatocellular carcinoma. *Metab Clin Exp*. 2016;65(8):1151–1160. doi:10.1016/j.metabol.2016.01.010
4. Alexander J, Torbenson M, Wu TT, Yeh MM. Non-alcoholic fatty liver disease contributes to hepatocarcinogenesis in non-cirrhotic liver: a clinical and pathological study. *J Gastroenterol Hepatol*. 2013;28(5):848–854. doi:10.1111/jgh.12116
5. Tabrizian P, Roayaie S, Schwartz ME. Current management of hepatocellular carcinoma. *World J Gastroenterol*. 2014;20(30):10223–10237. doi:10.3748/wjg.v20.i30.10223
6. Nakagawa S, Wei L, Song WM, et al. Molecular liver cancer prevention in cirrhosis by organ transcriptome analysis and lysophosphatidic acid pathway inhibition. *Cancer Cell*. 2016;30(6):879–890. doi:10.1016/j.ccell.2016.11.004
7. Bach DH, Lee SK, Sood AK. Circular RNAs in cancer. *Mol Ther Nucleic Acids*. 2019;16:118–129. doi:10.1016/j.omtn.2019.02.005
8. Mercer TR, Gerhardt DJ, Dinger ME, et al. Targeted RNA sequencing reveals the deep complexity of the human transcriptome. *Nat Biotechnol*. 2011;30(1):99–104. doi:10.1038/nbt.2024
9. Panda AC, Grammatikakis I, Kim KM, et al. Identification of senescence-associated circular RNAs (SAC-RNAs) reveals senescence suppressor CircPVT1. *Nucleic Acids Res*. 2017;45(7):4021–4035. doi:10.1093/nar/gkw1201
10. Zhao ZJ, Shen J. Circular RNA participates in the carcinogenesis and the malignant behavior of cancer. *RNA Biol*. 2017;14(5):514–521. doi:10.1080/15476286.2015.1122162
11. Yao Z, Xu R, Yuan L, et al. Circ_0001955 facilitates hepatocellular carcinoma (HCC) tumorigenesis by sponging miR-516a-5p to release TRAF6 and MAPK11. *Cell Death Dis*. 2019;10(12):945. doi:10.1038/s41419-019-2176-y
12. Tian F, Yu C, Wu M, Wu X, Wan L, Zhu X. MicroRNA-191 promotes hepatocellular carcinoma cell proliferation by has_circ_0000204/miR-191/KLF6 axis. *Cell Prolif*. 2019;52(5):e12635. doi:10.1111/cpr.12635
13. Wang YG, Wang T, Ding M, Xiang SH, Shi M, Zhai B. hsa_circ_0091570 acts as a ceRNA to suppress hepatocellular cancer progression by sponging hsa-miR-1307. *Cancer Lett*. 2019;460:128–138. doi:10.1016/j.canlet.2019.06.007
14. Liu BH, Zhang BB, Liu XQ, Zheng S, Dong KR, Dong R. Expression profiling identifies circular RNA signature in hepatoblastoma. *Cell Physiol Biochem*. 2018;45(2):706–719. doi:10.1159/000487163
15. Berindan-Neagoe I, Monroig Pdel C, Pasculli B, Calin GA. MicroRNAome genome: a treasure for cancer diagnosis and therapy. *CA Cancer J Clin*. 2014;64(5):311–336. doi:10.3322/caac.21244
16. Bertoli G, Cava C, Castiglioni I. MicroRNAs: new biomarkers for diagnosis, prognosis, therapy prediction and therapeutic tools for breast cancer. *Theranostics*. 2015;5(10):1122–1143. doi:10.7150/thno.11543
17. Adams BD, Kasinski AL, Slack FJ. Aberrant regulation and function of microRNAs in cancer. *Curr Biol*. 2014;24(16):R762–R776. doi:10.1016/j.cub.2014.06.043
18. Zeng XC, Liu FQ, Yan R, et al. Downregulation of miR-610 promotes proliferation and tumorigenicity and activates Wnt/beta-catenin signaling in human hepatocellular carcinoma. *Mol Cancer*. 2014;13:261. doi:10.1186/1476-4598-13-261
19. Palanisamy V, Jakymiw A, Van Tubergen EA, D'Silva NJ, Kirkwood KL. Control of cytokine mRNA expression by RNA-binding proteins and microRNAs. *J Dent Res*. 2012;91(7):651–658. doi:10.1177/0022034512437372
20. Wu J, Du X, Li W, et al. A novel non-ATP competitive FGFR1 inhibitor with therapeutic potential on gastric cancer through inhibition of cell proliferation, survival and migration. *Apoptosis*. 2017;22(6):852–864. doi:10.1007/s10495-017-1361-7
21. Gao G, Tian Z, Zhu HY, Ouyang XY. miRNA-133b targets FGFR1 and presents multiple tumor suppressor activities in osteosarcoma. *Cancer Cell Int*. 2018;18:210. doi:10.1186/s12935-018-0696-7
22. Zhang J, Li J, Li S, Zhou C, Qin Y, Li X. miR802 inhibits the aggressive behaviors of nonsmall cell lung cancer cells by directly targeting FGFR1. *Int J Oncol*. 2019;54(6):2211–2221. doi:10.3892/ijo.2019.4765
23. Blum HE. Molecular therapy and prevention of hepatocellular carcinoma. *Hepatobiliary Pancreat Dis Int*. 2003;2(1):11–22.
24. Villani R, Vendemiale G, Serviddio G. Molecular mechanisms involved in HCC recurrence after direct-acting antiviral therapy. *Int J Mol Sci*. 2018;20(1):49. doi:10.3390/ijms20010049
25. Kristensen LS, Hansen TB, Veno MT, Kjems J. Circular RNAs in cancer: opportunities and challenges in the field. *Oncogene*. 2018;37(5):555–565. doi:10.1038/onc.2017.361
26. Liu L, Yang X, Li NF, Lin L, Luo H. Circ_0015756 promotes proliferation, invasion and migration by microRNA-7-dependent inhibition of FAK in hepatocellular carcinoma. *Cell Cycle*. 2019;18(21):2939–2953. doi:10.1080/15384101.2019.1664223
27. Sun B, Gu X, Chen Z, Xiang J. MiR-610 inhibits cell proliferation and invasion in colorectal cancer by repressing hepatoma-derived growth factor. *Am J Cancer Res*. 2015;5(12):3635–3644.
28. Wang J, Zhang J, Wu J, et al. MicroRNA-610 inhibits the migration and invasion of gastric cancer cells by suppressing the expression of vasodilator-stimulated phosphoprotein. *Eur J Cancer*. 2012;48(12):1904–1913. doi:10.1016/j.ejca.2011.11.026
29. Yan Y, Peng Y, Ou Y, Jiang Y. MicroRNA-610 is downregulated in glioma cells, and inhibits proliferation and motility by directly targeting MDM2. *Mol Med Rep*. 2016;14(3):2657–2664. doi:10.3892/mmr.2016.5559
30. Wang L, Bo X, Zheng Q, Xiao X, Wu L, Li B. miR-296 inhibits proliferation and induces apoptosis by targeting FGFR1 in human hepatocellular carcinoma. *FEBS Lett*. 2016;590(23):4252–4262. doi:10.1002/1873-3468.12442
31. Takano M, Shimada K, Fujii T, et al. Keratin 19 as a key molecule in progression of human hepatocellular carcinomas through invasion and angiogenesis. *BMC Cancer*. 2016;16(1):903. doi:10.1186/s12885-016-2949-y
32. Matsuki M, Hoshi T, Yamamoto Y, et al. Lenvatinib inhibits angiogenesis and tumor fibroblast growth factor signaling pathways in human hepatocellular carcinoma models. *Cancer Med*. 2018;7(6):2641–2653. doi:10.1002/cam4.1517
33. Hoshi T, Watanabe Miyano S, Watanabe H, et al. Lenvatinib induces death of human hepatocellular carcinoma cells harboring an activated FGF signaling pathway through inhibition of FGFR-MAPK cascades. *Biochem Biophys Res Commun*. 2019;513(1):1–7. doi:10.1016/j.bbrc.2019.02.015